Contractional deformation of porous sandstone: Insights from the Aztec Sandstone, SE Nevada, USA

Contractional deformation of porous sandstone: insights from the Aztec Sandstone in the footwall to the Sevier-age Muddy Mountains thrust, SE Nevada, USA

Haakon Fossen[a, b*], Luisa F. Zuluaga[d,a], Gregory Ballas[c],

Roger Soliva[c], Atle Rotevatn[a],

[a] *Department of Earth Science, University of Bergen, Allégaten 41, N-5007 Bergen, Norway.*

[b] *Museum of Natural History, University of Bergen, Allégaten 41, Postboks 7800, N-5020 Bergen, Norway.*

[c] *Laboratoire Géosciences Montpellier, University Montpellier, Place Eugène Bataillon, 34000 Montpellier, France*

[d] *Centre for Integrated Petroleum Research (Uni Research CIPR) Allégaten 41, 5007 Bergen, Norway*

Abstract

Contractional deformation of highly porous sandstones is poorly explored, as compared to extensional deformation of such sedimentary rocks. In this work we explore the highly porous Aztec Sandstone in the footwall to the Muddy Mountain thrust in SE Nevada, which contains several types of deformation bands in the Buffington tectonic window: 1) Distributed centimeter-thick shear-enhanced compaction bands (SECBs) and 2) rare pure compaction bands (PCBs) in the most porous parts of the sandstone, cut by 3) thin cataclastic shear-dominated bands (CSBs) with local slip surfaces. Geometric and kinematic analysis of the SECBs, the PCBs and the majority of the CSBs shows that they formed during ~E-W (~N100E)

* Corresponding author (haakon.fossen@geo.uib.no)

shortening, consistent with Sevier thrusting. Based on stress path modeling, we suggest that the compactional bands (PCBs and SECBs) formed during contraction at relatively shallow burial depths, before or at early stages of emplacement of the Muddy Mountains thrust sheet. The younger cataclastic shear bands (category 3), also related to E-W Sevier thrusting, are thinner and show larger shear offsets and thus more intense cataclasis, consistent with the initiation of cataclastic shear bands in somewhat less porous materials. Observations made in this work support earlier suggestions that contraction lead to more distributed band populations than what is commonly found in the extensional regime, and that shear-enhanced compaction bands are widespread where porosity is high.

Keywords: Sevier thrusting; porous sandstone deformation; deformation bands; contractional deformation

---

1. Introduction

Sandstones with porosity in excess of ca. 15% generally develop deformation bands during low-strain deformation. The evolution of deformation bands during extensional tectonics has been extensively studied since the late 70s, particularly through investigations of deformed Jurassic sandstones of the Colorado Plateau (e.g., Aydin and Johnson, 1978; Antonellini and Aydin, 1994). The type of deformation band most commonly reported in the literature show shear-induced grain crushing and compaction in a 1-2 mm thick zone in the sandstone with up to a few cm of shear offset (e.g., Aydin and Johnson, 1978; Underhill and Woodcock, 1987; Antonellini and Aydin, 1994; Davis, 1999). Such bands are referred to as compactional shear

bands (Fossen et al., 2007) or, combining their textural and kinematic characteristics, *cataclastic compactional shear bands* (CSBs). In addition, non-cataclastic bands with predominantly shear offsets are very common in the extensional regime, particularly where the burial depth at the time of deformation was low (<1 km) (Fisher and Knipe, 2001; Hesthammer and Fossen, 2001). A characteristic feature of sandstone deformation in the extensional regime is the tendency for deformation bands to cluster into zones that evolve into faults with deformation band damage zones (Antonellini and Aydin, 1994; Shipton and Cowie, 2003, Johansen and Fossen, 2008).

Much less work has been done on deformation of highly porous sandstones during contraction. It appears that in addition to mm-thick cataclastic (compactional) shear bands (CSBs) there are two additional types of structures found in the contractional or thrusting regime, known as *shear-enhanced compaction bands* (SECBs) and *pure compaction bands* (PCBs) (Eichhubl et al., 2010; Fossen et al., 2011; Ballas et al., 2013). Both types of structures are reported from the Valley of Fire State Park, Nevada (Sternlof et al., 2005; Tembe et al., 2008), where they both were called compaction bands until Eichhubl (2010) suggested that they are kinematically different, and therefore relate differently to principal axes of stress and strain. Specifically, PCBs form perpendicular to the shortening direction or the maximum compressional stress direction σ_1, while SECBs form oblique to this direction, typically in the form of two conjugate sets bisected by σ_1 (Fig. 1). SECBs are notably thicker (cm-scale) than the mm-thick cataclastic bands (CSBs) widely reported from extensional settings, and show much smaller (typically less than 1 mm) shear offsets that are quantitatively comparable to the compaction-induced offsets (Eichhubl, 2010). It has also been

suggested that shortening of porous sandstones generates more distributed arrays of bands than what is typically seen in the extensional regime (Solum et al., 2010). This was explored in detail by Ballas et al. (2012 and 2013), who studied poorly consolidated porous sandstones in Provence, France. In this area, extensional deformation generated deformation band clusters that developed into normal faults, whereas the preceding contraction created much more evenly distributed SECBs and CSBs without any obvious relationship to faults (Saillet and Wibberley, 2010 ; Soliva et al., 2013).

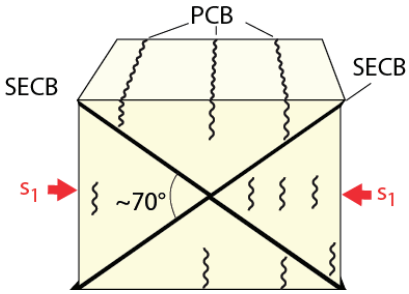

Figure 1. The spatial relationship between pure compaction bands (PCB), shear-enhanced compacion bands (SECB) and the maximum principal stress direction.

In the present contribution we will examine an area where porous Aztec Sandstone has been shortened and overridden by a several kilometer thick Sevier-age thrust sheet. The aim is to explore how porous sandstone responds to contractional deformation that leads to the emplacement of a thrust nappe on top of the sandstone, and to add to our understanding of sandstone deformation in the contractional regime in general. For a discussion of the deformation along the thrust fault itself, see Brock and Engelder (1977).

2. Geologic setting

The focus of this study is the Jurassic Aztec Sandstone, which is part of an extensive eolian sandstone unit called the Navajo and Nugget sandstones on the Colorado Plateau to the east and north. The Aztec Sandstone was involved in Sevier thrusting in Nevada and western Utah, and is exposed in the tectonic Buffington window underneath Paleozoic rocks of the Muddy Mountains thrust sheet (Fig. 2), and in the Valley of Fire State Park to the north-east (Fig. 3).

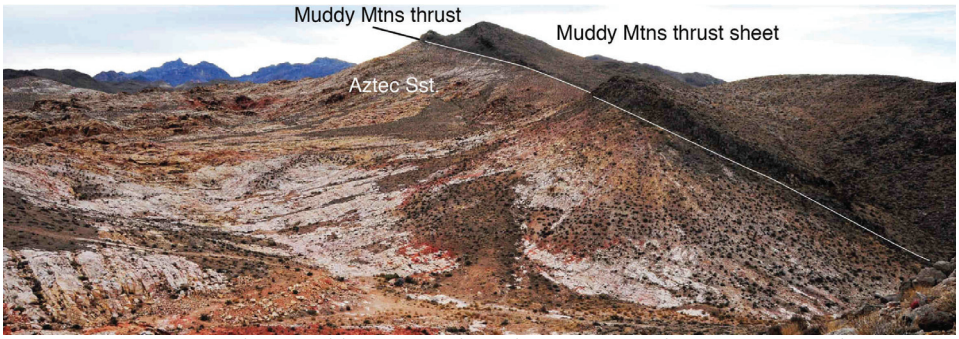

Figure 2: The Muddy Mountains thrust, separating Aztec Sandstone (footwall) from Paleozoic carbonate-rich rocks in the hanging wall (right). The contact has been rotated during Basin and Range normal faulting.

The primary study area is the Buffington tectonic window, which exposes around 28 km^2 of porous Aztec Sandstone underneath the Muddy Mountains thrust. The thrust contact against mostly dolomites and limestones of the Bonanza King Formation in the lower part of the overlying thrust sheet is described by Brock and Engelder (1977). In short, the Aztec sandstone has developed a meter-thick zone of strong cataclastic deformation and grain pressure solution that reduce porosity to almost zero along the contact. However, some meters or tens of meters downwards into the sandstone it reaches porosities up to 20-25% and permeabilities of several darcy.

Following the Sevier contraction, the region was affected by Basin and Range extensional tectonics, as manifested by a large number of extensional faults offsetting the Muddy Mountains thrust contact and tilting the thrust and the Aztec Sandstone (Fig. 3). Transcurrent fault systems, notably the Las Vegas Valley shear zone, accompanied the Basin and Range extension, but had only limited influence on the Buffington Window area. The general current dip of the Aztec Sandstone in the window is around 20° to the southeast, implying that pre-Cenozoic structures should be rotated correspondingly.

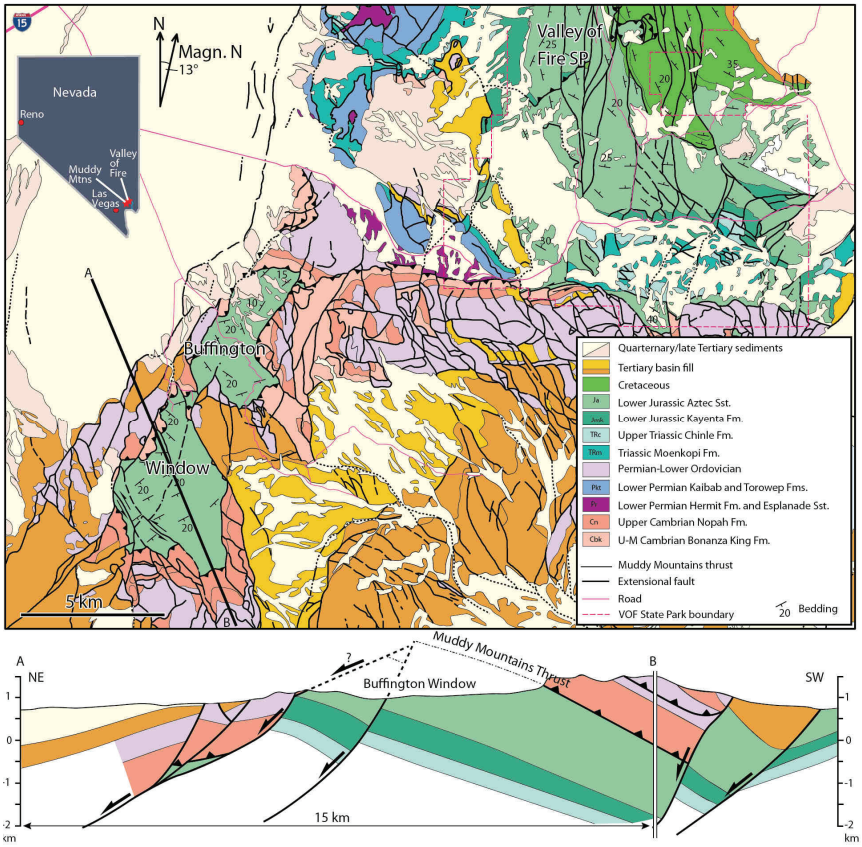

Figure 3: Geologic map and cross section of the Buffington Window and Valley of Fire area, SE Nevada. Based on Bohannon (1983).

3. Structural observations

The Aztec Sandstone in the Buffington Window exhibits three distinctly different types of deformation bands; pure compaction bands (PCBs), shear-enhanced compaction bands (SECBs) and cataclastic compactional shear bands (CSBs). These band types are distinguished on the basis of geometry, kinematics, thickness and deformation mechanisms.

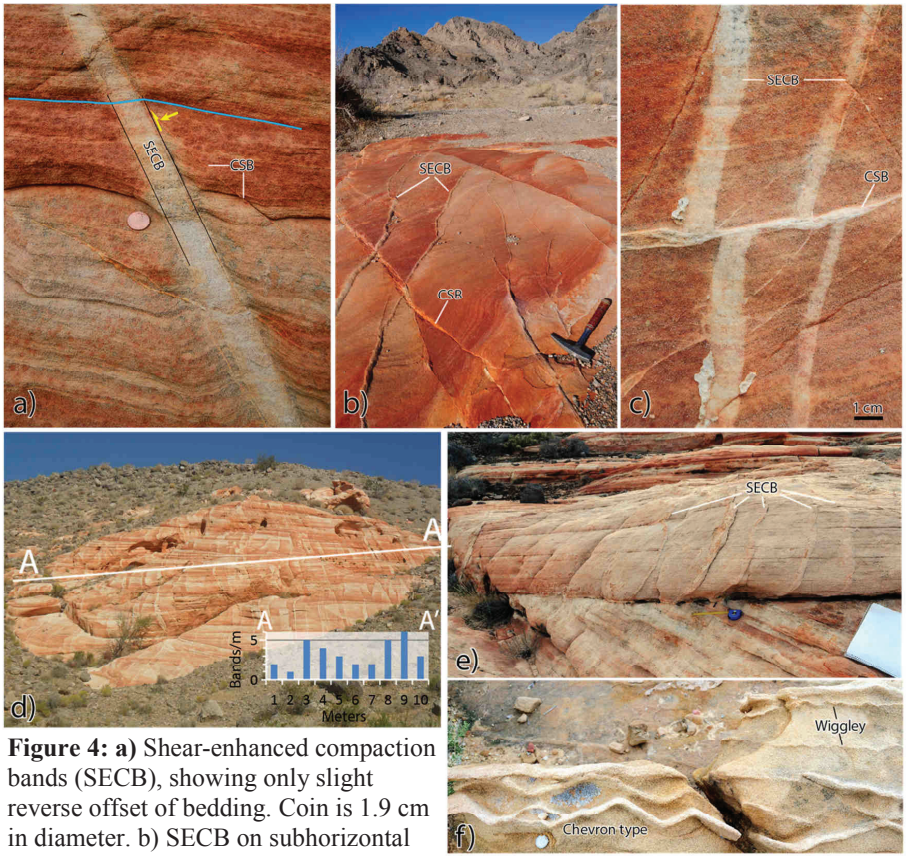

Figure 4: a) Shear-enhanced compaction bands (SECB), showing only slight reverse offset of bedding. Coin is 1.9 cm in diameter. b) SECB on subhorizontal surface, showing evidence of growth by linkage. c) Thin zone of cataclastic shear bands (CSBs) offsetting two SEDBs. d) Population of SECBs with an average spacing around $3m^{-1}$. e) A parallel set of planar SECB limited to the highly porous/permeable lower part of a dune unit. f) Wiggley and chevron types of pure compaction bands, Valley Of Fire.

Pure compaction bands

Structures recognized as PCBs in the Buffington Window - Valley of Fire area are 0.5-2 cm thick bands characterized by non-planar geometries, commonly showing wiggly or chevron-style geometries (Fig. 4f). No offset is seen across PCBs, and they are only observed sporadically in the most porous and permeable parts of the Aztec sandstone. On the microscale, PCBs involve only a limited amount of cataclasis, similar to CSBs described from Valley of Fire (Eichhubl et al., 2010), but somewhat less than those described from southern Utah (Mollema and Antonellini, 1996; Fossen et al., 2011). They are somewhat more common in highly porous and permeable layers in Valley of Fire (close to 25% porosity as estimated from thin sections, and 15 Darcy permeability based on measurements using a portable probe permeameter (TinyPerm-II); see Rotevatn et al. 2008 for details on the method). The PCBs form high angles to bedding and dip steeply to the WNW throughout the Buffington Window area (Figs. 5 and 6), with very similar orientations to those found in the Valley of Fire (compare Figs. 5a and d). This orientation is consistent with an ESE-WSW shortening direction (see below).

Shear-enhanced compaction bands

The SECBs are cm-thick structures that typically show a very planar geometry (Fig. 4a, c, d and e), although curvature related to linkage structures can sometimes be seen in horizontal sections (Fig. 4b). They record very small (mm-scale or less) offsets that may be difficult to see, depending on their orientation with respect to the local lamination. Where offset is seen it appears reverse in cross-section (Fig. 4a). Microstructurally they show clear evidence of cataclasis, but also pressure solution can

be important (Figs. 7 and 8a-b); hence, they reduce porosity and permeability. Probe permeameter measurements of host rock and band permeability suggest variable permeability reductions by SECBs, from close to none to 2.8 orders of magnitude in bands where dissolution is prominent (Fig. 9). These observations are similar to SECBs measured in Buckskin Gulch, Utah by Fossen et al. (2011).

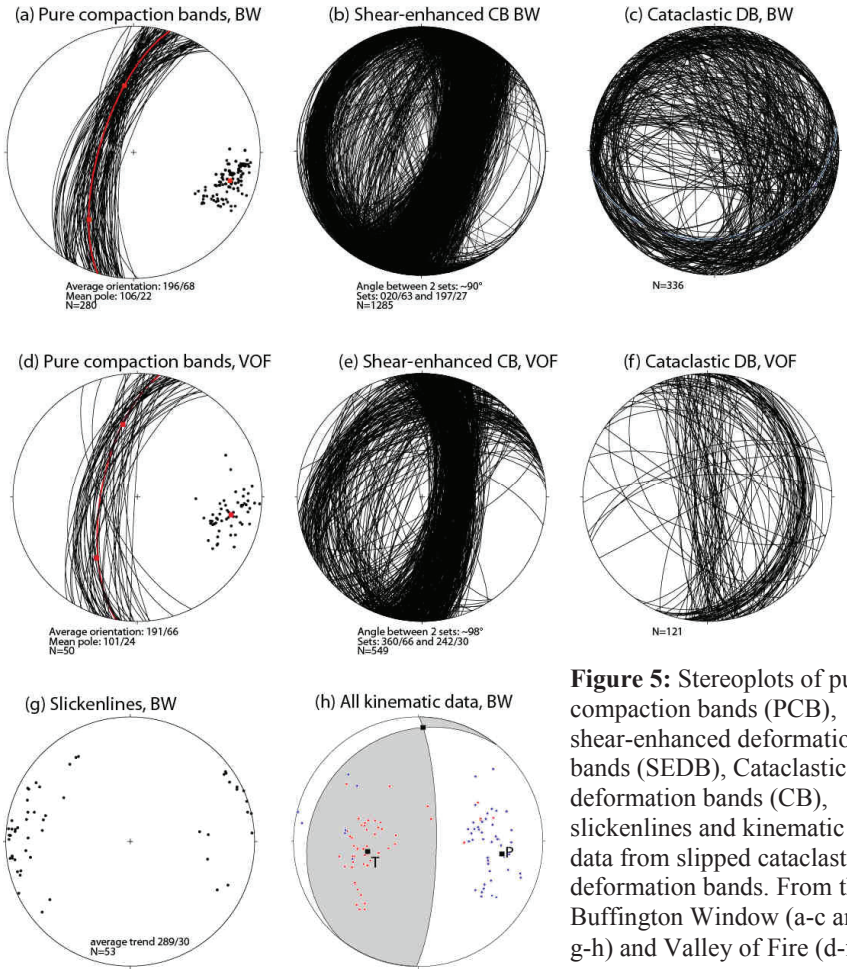

Figure 5: Stereoplots of pure compaction bands (PCB), shear-enhanced deformation bands (SEDB), Cataclastic deformation bands (CB), slickenlines and kinematic data from slipped cataclastic deformation bands. From the Buffington Window (a-c and g-h) and Valley of Fire (d-f)

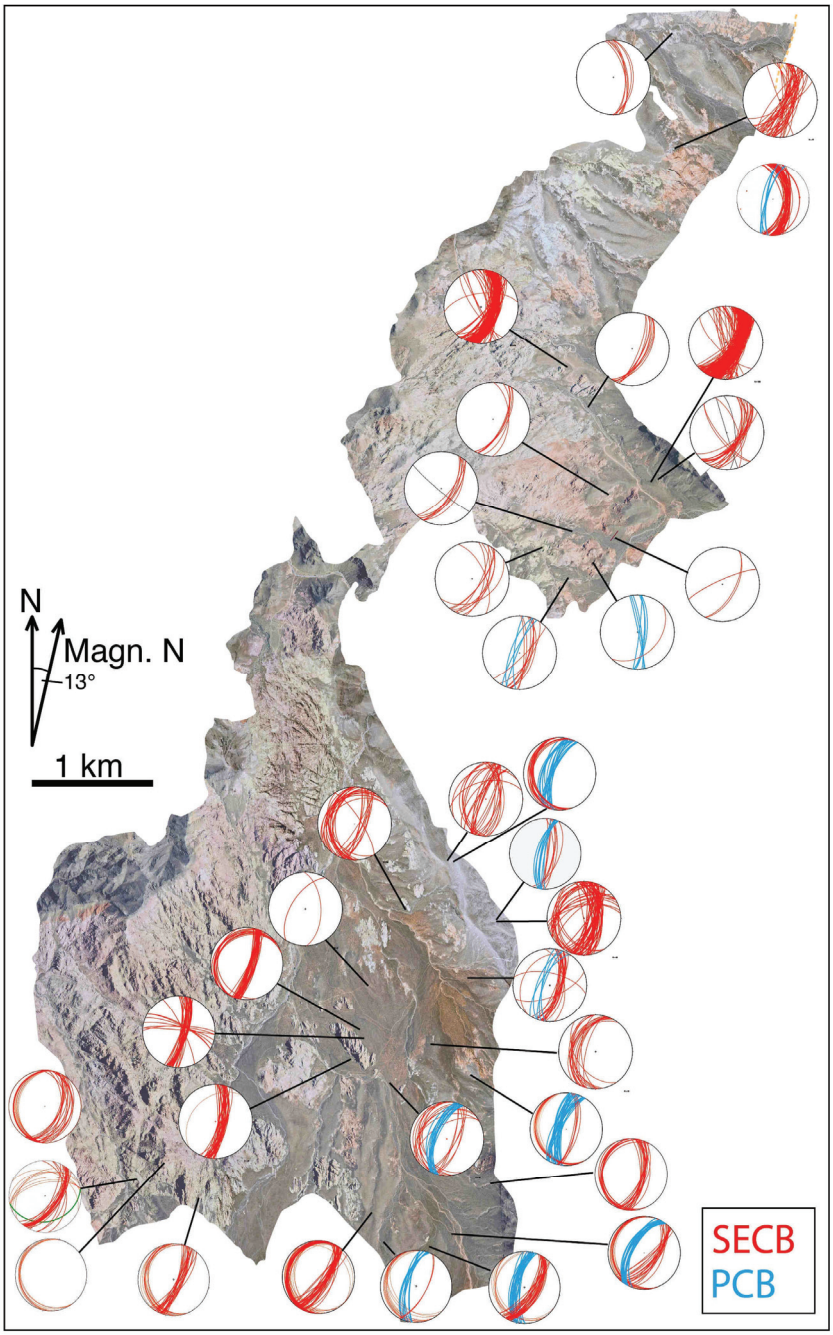

Figure 6: Aerial photo of the Buffington Window with stereonet plots of SECB (shear-enhanced compaction bands) and PCB (pure compaction bands) orientations from selected localities.

The SECBs define two sets, where the majority of the SECBs dip steeply to the ESE (020/63E on average). This dominant set can be observed along several ten-meters long outcrops as quite well organized network showing an average band thickness of

about 11.6 ± 7.6 mm (N = 41), an average band spacing of about 0.315 ± 0.2268 m (N = 40) and a corresponding average band density of 3.3 bands/m (Fig. 4d). The other set is less well defined, and dips in the opposite direction (approximately 197/27W). The bands of this set are sometimes observed parallel to dune foreset lamina similar to SECBs described by Mollema & Antonellini (1996) in southern Utah and by Aydin & Ahamadov (2009) in the Valley of Fire area. Some variations are seen between different localities (Fig. 6), and at some outcrops the bands show a variation in strike that in part can be related to band growth by segment linkage (SECB in Fig. 4b). These variations are reflected by the scatter portrayed in the stereoplots (Figs. 5b and 6). The conjugate sets are generally observed separately in different dune sets, as described by Deng & Aydin (2012) at Valley of Fire, whereas only a few dunes show both sets.

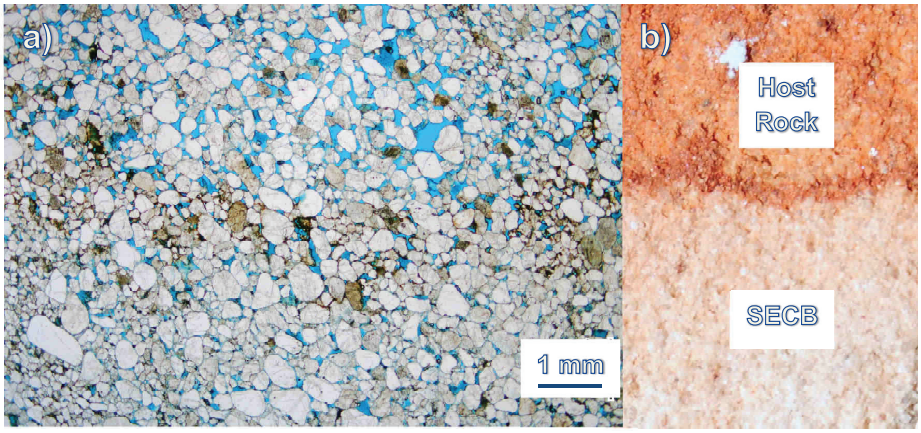

Figure 7: Boundary between matrix and SECB as observed in thin section and hand sample. Note the reduction in porosity (blue color) in the SECB.

Cataclastic compactional shear bands

Cataclastic compactional shear bands (CSBs), i.e. cataclastic bands with predominantly shear displacement, are around 1 mm thick and show cm-scale reverse offsets that consistently postdate the PCBs and SECBs (Fig. 4c). Some CSBs get

deflected close to SECBs, bending into parallelism with the SECB and following their margins, while others cut straight through. They show a fairly wide range of orientations, many of which define low-angle structures (Fig. 5f). They are observed sporadically in the window where porous sandstones are observed, also in foresets of dunes where SECBs and PCBs are not observed, without any well-defined network organization. Dipping bands generally show reverse offsets and two conjugate sets with a dihedral angle of about 60°, consistent with a contractional regime. These bands are sometimes specifically located at dune boundaries or dune foresets. Locally there are steep bands that offset the reverse bands, and it is possible that these steep bands may represent a later (Basin and Range?) phase of deformation. CSBs also organize themselves occasionally into ladder structures (Davis, 1999; Schultz and Balasko, 2003) that show reverse offset.

At the microscale, these CSBs show much stronger internal cataclasis than the PCBs and SECBs (Fig. 8c). Furthermore, some of the bands have developed an internal slip surface, where grain crushing is very intense (cf. Rotevatn et al. 2008). Locally they also develop into faults containing internal gouge and intense cataclasis at the boundaries of certain sand dune units. These slip surfaces exhibit striations or slickenlines from mechanically broken grains, which together with the observation of sense of slip on bands and faults can be used to constrain the shortening direction during their formation (see Section 4 below).

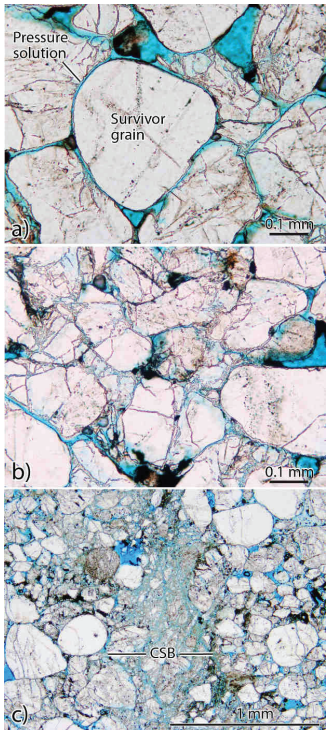

Figure 8: Internal structure of SECB (a and b), showing dissolution and evidence for some grain fracture. c) Thin section view of cataclastic shear band, showing much more profound grain crushing than SECB.

4. Strain and shortening direction

Deformation bands, particularly PCBs and SECBs, are low-strain features. Also, the strain that they accommodate in the study area as a whole is very low (<0.25%), notwithstanding the fact that the sandstone has been overthrust by a large thrust sheet. Nevertheless, the deformation bands and their orientations provide information about the direction of maximum shortening. The SECBs, which formed before the CSB, show a fairly consistent pattern with a dominant E-dipping set and a subordinate W dipping one (Figs. 5 and 6). The PCBs (Fig. 5a) define a single set that seems to bisect the two sets of SECBs. Hence, SECBs and PCBs together form a consistent geometric arrangement that indicates maximum shortening along a direction plunging 24 degrees toward 101. Considering the overall E-tilted bedding caused primarily by post-Sevier

Basin and Range extensional faulting, restoration of bedding to horizontal suggests an approximately horizontal shortening direction at around N100E for the Aztec sandstone both in the Buffington Window and Valley of Fire.

Some of the CSBs show central striated slip surfaces that serve as kinematic indicators. Several are parallel or make a low angle to bedding, which means that sense of slip may be difficult to determine with confidence. However, many of the striations are E-W oriented (Fig. 5g), suggesting E-W shortening, and this is supported by kinematic analysis of the slip data and the dihedral angle defined by conjugate sets (Fig. 5h). Hence, the CSBs exhibit an almost E-W shortening direction, which corresponds quite well with that extracted from the SECB and PCB orientation data.

5. Discussion and conclusions

The Jurassic Aztec sandstone in the Buffington Window, SE Nevada, is an example of porous sandstone overthrust by a nappe of older rocks in an orogenic foreland setting. The internal strain in the sandstone is very low, except for a relatively narrow zone along the Muddy Mountains thrust. It is not clear why the deformation is so strongly localized to the thrust zone. As argued by Hubbert and Rubey (1959), high fluid pressures help thrust nappes advance above their footwalls due to the related reduction in fault strength along their base. Evidence for elevated pore pressure within the thrust zone during thrusting is represented by hydraulic breccia in hanging-wall carbonates along the thrust faults. Breccia structures are also present in the Aztec Sandstone in the form of vertical structures some decimeters to meters wide, although these may be more local pressure-controlled structures. Hence some overpressure must

have occurred, at least locally. It is not clear if shalely layers in the carbonate-dominated rocks of the thrust nappe and/or the cataclastic and cemented thrust zone facilitated overpressure for sufficiently long periods of time that the thrust sheet could move – transport of a major thrust nappe over a thick permeable unit like the Aztec Sandstone remains enigmatic (Brock and Engelder, 1977). Regardless, mild strains are distributed also in the footwall in the form of different types of deformation bands, as further discussed below.

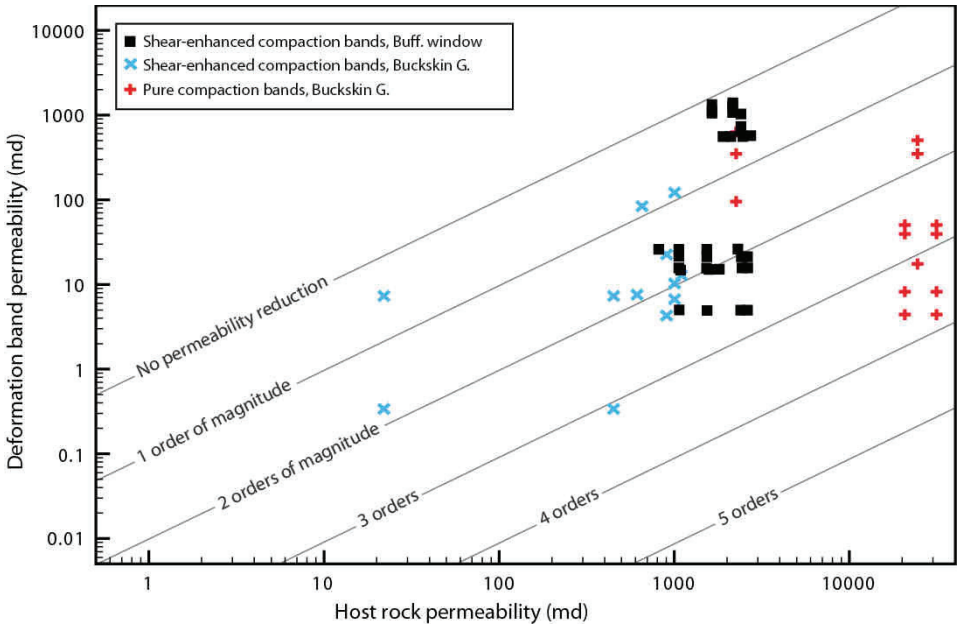

Figure 9: Permeability measurements of shear enhanced compaction bands (SECB), Buffington Window, plotted together with measurements of SECB and compaction bands from the Buckskin Gulch area, Utah (Fossen et al., 2011).

Distribution of bands in a contractional stress-state

The close to E-W shortening direction reflected by all groups of deformation bands in the Aztec sandstone is in good agreement with the Sevier shortening direction reported from this part of the Cordilleran thrust belt (DeCelles, 2004). In general, the

present work fit what seems to be a general pattern of contractional deformation of porous sandstones: widely distributed deformation band populations and the formation of compaction bands in highly porous sand(stones). The widely distributed occurrence of SECBs in the Buffington Window and Valley of Fire rather than localization into dense band clusters is qualitatively similar to observations made by Solum et al. (2010), Soliva et al. (2013) and Ballas et al. (2014). Their occurrence is controlled by local lithologic parameters (porosity, grain size), but where they occur, they are more or less evenly distributed with a regular spacing, a bit similar to joint distributions in competent layers (e.g., Rives et al. 1992). While the spacing of SECBs in the Buffington Window is around 3 m^{-1}, it is considerably higher in some examples of the Provence sandstones investigated by Soliva et al. (2013) and Ballas et al. (2014) (ca. 30 m^{-1}), implying a lower strain level in the Buffington Window (although the bands are thicker in the Buffington Window). To what extent the spacing of SECBs relates to bed thickness (effective bed thickness is much higher for the Aztec Sandstone), rock properties, and/or boundary conditions remains to be investigated. Chemenda et al. (2014) found that spacing also correlates with symmetry in the sense that a double set of bands (high symmetry) develops more widely spaced bands than layers with only one set of bands. For PCBs field observations show that for the Navajo Sandstone, the band density increases consistently with an increase in grain size, porosity and permeability (Fossen et al., 2011).

So far, shear-enhanced compaction bands (SECBs) and pure compaction bands (PCBs) have only been reported from contractional settings, notably Valley of Fire, Nevada (Sternlof et al., 2005; Eichhubl et al., 2010), Buckskin Gulch, Utah (Mollema &

Antonellini, 1996; Fossen et al., 2011), and Provence, France (Ballas et al., 2013). Following Soliva et al. (2013), an explanation for this is the low differential stress associated with the contractional (or thrust) regime at shallow crustal levels. Soliva et al. (2013) discussed this in the framework of the differential stress vs. the effective mean stress, known as the q-p diagram (Fig. 10a), which is commonly used to represent state of stress and mode of deformation (e.g., Schultz & Siddharthan, 2005). This diagram is composed of a linear envelope for frictional sliding (critical state line), and an elliptical envelope or cap for compactional flow. Permanent deformation (plastic yielding) occurs when the stress path intersects the yield cap or the critical state line. The elliptical shape of the cap is defined experimentally (e.g., Zhang et al. 1990; Wong et al., 1997; 2012; Grueschow and Rudnicki, 2005), and this experimental work has shown that its intersection P* with the horizontal p-axis (Fig. 10a) depends on grain radius R and porosity ϕ through the relation $P^* = (\phi R)^{-1.5}$. In concert with Soliva et al. (2013), we follow Rudnicki (2004) and define the cap geometry as a quarter ellipse with an aspect ratio $a/b=1.74$, where a is the maximum value of q and $b=P^*/2$. Hence, the position of the cap in the q-p diagram is defined by the local lithology (grain size and porosity), whereas the stress path is controlled by the amount of overburden (burial depth) and tectonic stress.

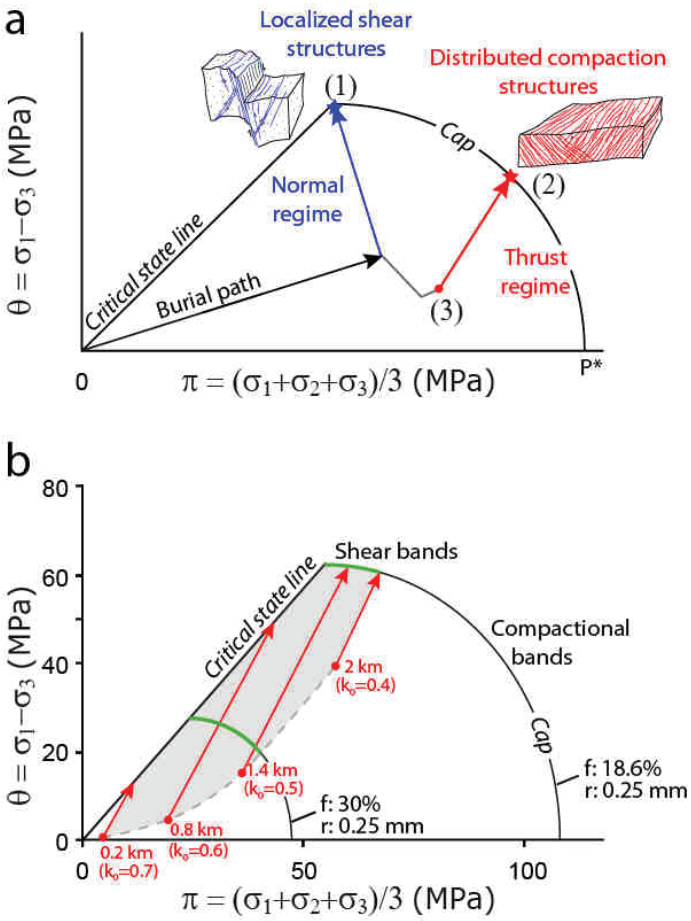

Figure 10: a) Generalized q-p diagram with a theoretical stress path for a highly porous sand(stone) undergoing burial and then normal fault regime (blue line) or thrust regime (red line) stress evolution. Normal fault regime implies a reduction in the horizontal stress, and the path intersects the upper part of the cap (1), implying shearing. In the thrusting regime the cap is intersected in the area where compaction is important (2). b) Stress paths (corresponding to red path in a) for the thrusting regime for four cases of different burial depth and elastic properties. Two caps for porosities of 30% and 18.6% are indicated, and it is seen that SEDBs can more easily form in the high porosity case where the sector of possible cap intersections (green line) is wider. See text for discussion.

The mode of deformation at the onset of permanent deformation is prescribed by the point at which the stress path intersects the cap. The mode is compactional (PCBs and SECBs) in the middle part of the cap, while it is dominated by simple shear (CSBs) near the intersection between the cap and the critical state line. The expected stress

path for a buried sandstone deformed in the contractional (or thrust) regime is one that reaches the yield cap in its central part (Fig. 10a). In contrast, the extensional (normal fault) regime predicts a point of intersection higher on the cap, i.e. closer to simple shear (Soliva et al., 2013) (Fig. 10a). Hence, according to this simple model, deformation bands forming in the normal regime should be shear-dominated, while they should be more compactive (SECBs and CSBs) and distributed in the contractional regime, i.e. similar to what is generally observed. The difference in localization is likely related to the amount of shear involved: numerous studies have documented clustering of shear deformation bands into zones that may or may not evolve into faults or slip surfaces, while contraction, which involves more compaction, result in much more distributed bands. However, it is interesting to note that even the cataclastic bands in the Aztec Sandstone do not localize easily into well-defined fault structures in the area, except for specific conditions such as at dune boundaries, but appear to be distributed in the sandstone. Hence there may also be other conditions, including boundary conditions that control the distribution of bands.

In order to utilize the q-p diagram more specifically for the Buffington Window area, we want to consider the stress conditions and rock properties at the time of deformation of the Aztec Sandstone. As a relatively well-sorted eolian sandstone unit we can assume that the porosity was high (perhaps 30%) at shallow burial depths, decreasing to the present conditions over time due to mechanical compaction and dissolution at grain contact points. However, the burial depth at the time of deformation band formation is not clear. As discussed by Brock and Engelder (1977),

local clastic sediments occur between the Keystone-Muddy Mountains thrust and the Aztec Sandstone (footwall), with clasts from both Mezosoic sandstones and carbonates similar to those found in the Muddy Mountains nappe. This has led several authors to suggest that the thrust sheet moved across the earth's surface, represented by an erosional top Aztec Sandstone covered by debris from the advancing thrust sheet, i.e., a foreland basin. The thickness of this basin is unknown, but considered to be relatively thin because of the limited amounts (up to a few tens of meters) preserved in the Buffington Window (Brock and Engelder, 1977). Hence, the burial depth at the onset of contraction is uncertain, but could be very shallow, depending on the local thickness of the Sevier foreland basin. The maximum burial depth, on the other hand, is controlled by the thickness of the thrust sheet, which from stratigraphic considerations has been estimated to a minimum of 4-5 km (Brock and Engelder, 1977).

In an attempt to constrain the depth of deformation band formation, we have calculated the stress paths for the thrust regime for different cases, i.e. stress paths that initiates once the maximum horizontal stress exceeds the vertical stress and the thrust regime is entered (point (3) in Fig. 10a). This was done for the following burial depths: 0.2, 0.8, 1.4 and 2.0 km (Fig. 10b), using appropriate ratios k_0 of horizontal vs. vertical effective stress, which relates to the state of compaction of the sandstone, especially due to pressure solution and thus to the burial depth (see Soliva et al., 2013 and references therein). The extreme burial depth values chosen were 0.2 and 2 km, and these define a space of possible thrust-domain stress conditions for the sandstone (Fig.

10b, shaded area). Two caps are considered that relate to the parts of the Aztec Sandstone where SECBs are found: one for shallow burial conditions (30% porosity, grain radius of 0.25 mm) and one for maximum burial conditions (18.6%, which is the estimated current porosity, and the same grain radius of 0.25 mm). A large part of this porosity reduction is by pressure solution, which occurs at significant rates at temperatures ≥ 90 °C (Bjørkum et al., 1998). Hence the cap calculated for 18.6% porosity is relevant to band formation at 2-3 km burial depth and low values of k_0 (0.4), while the one calculated for 30% porosity is relevant for shallower burial and large values of k_0 (0.7). In either case, the sector of each cap that can be intersected by the stress paths is marked by a thicker green color. This sector of possible cap intersections is narrow and in the shearing-mode upper part of the cap for high burial depths (2 km), hence SECBs and PCBs are not expected to form at such burial depths. In contrast, for low burial depths and high (30%) porosity, this sector is much wider (about half the cap), suggesting that compactional bands (SECBs and PCBs) can form at these low burial conditions. Hence we conclude that the SECBs and PCBs most likely formed at relatively low burial depths, up to 1.4 km depth, which would imply that they formed before or at a relatively early stage of thrust sheet emplacement. However, the CSBs could have formed also at deeper burial depths, i.e. during overthrusting, consistent with the observed cross-cutting relationships (Figure 4c).

Organization of band network

The SECBs both in the Buffington Window and Valley of Fire are organized into networks consisting of conjugate sets in isolated parts of the sandstone reservoir,

typically with the E-dipping set being the dominating set. The fact that the E-dipping (foreland-dipping) conjugate set of SECBs is overall more pronounced than the W-dipping (hinterland-dipping) may seem surprising if they formed during E-directed overthrusting, in which case we may expect the dominant set of SECBs to be dipping toward the hinterland (west). In order to elucidate the causal mechanisms behind this situation, we draw parallels to similar SECB populations formed in poorly consolidated sandstones in Provence, France. These sandstones were deformed at shallow (<500 m) depths during mild regional contractional tectonics without the formation of major thrust nappes. SECBs in this area also form conjugate sets of bands, but where each set is largely confined to domains rather than both sets being present in the same outcrop (Ballas et al., 2013). These authors concluded that the establishment of a set of uniformly dipping bands must have had an impeding effect on oppositely dipping band, which would rather form in parts of the sandstone with no preexisting SECBs and that the dip direction of the bands is more or less arbitrary. A relationship between the dipping direction of SECBs and the foreset of dunes is however described by Deng & Aydin (2012). These authors suggest that the dipping direction is not necessarily arbitrary in the Aztec Sandstone but closely related to the anisotropy imposed by eolian cross beds. However, few of the sets in the Buffington Window directly follow eolian cross beds, hence the role of this anisotropy on set development is not immediately clear, and further exploration of this effect seems to require numerical modeling of such anisotropic sandstone.

Numerical modeling of homogeneous sandstone has been carried out by Chemenda et al. (2012 and 2014). They produced populations of oppositely dipping SECBs using lithological parameters that correspond to that of the Aztec Sandstone in the Valley of Fire area and CSBs or SECBs formation, respectively. These authors used a three-layer model where a 1 m elastic-plastic layer was confined between two 0.5 m elastic layers, and where layer-parallel shortening and layer-perpendicular extension was applied. An elastic–plastic instability resulted in the formation of SEDBs with symmetric or asymmetric arrangements, depending on the elastic properties of the layers and frictional properties of the layer boundaries. These numerical results demonstrate that it is possible to produce uniformly dipping bands (asymmetric distributions of SECBs) in the Aztec Sandstone during layer-parallel shortening (subhorizontal σ_1) (Fig. 11). In the case of the Aztec Sandstone, a difference in elasticity between dune foresets, because of their differences in grain size and porosity, could then lead to the formation of asymmetric SECB networks of the style observed in the study site. This hypothesis is supported by the formation of SECBs and PCBs in high-porosity foresets showing consequently lower elasticity whereas few or no bands are generally observed in foresets with finer grain size and lower porosity, and therefore higher elasticity. These models suggest also that a high friction at the contact between sandstone layers lead to the development of asymmetric band networks (Chemenda et al., 2014). The presence of SECBs or CSBs along the dune and foreset boundaries should increase the friction at the contact and then also lead to asymmetric network formation. The similarities to asymmetric SECB distributions in sandstones in Provence, which formed without thrusting, may suggest that these SECB populations

in the Aztec Sandstone also formed prior to thrusting. However, such an arrangement of SECBs could also have formed during thrusting, provided that the orientation of σ_1 in the footwall during thrusting was close to horizontal, which again would depend on the friction on the thrust fault during thrusting.

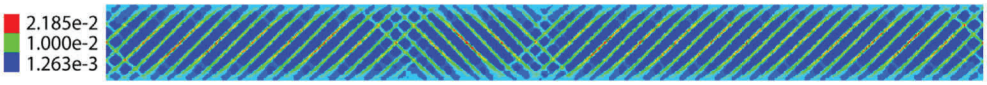

Figure 11: Output from a plane strain finite-difference three-layer model showing the 1 m thick middle elastic-plastic layer located between two 0.5 m thick elastic layers (not shown). Layer-parallel compression generated elastic–plastic instability that resulted in the formation of SEDBs with a preferred orientation. The figure shows variations in accumulated inelastic shear strain. Young's modulus is 10 GPa for all layers. From Chemenda et al. (2014).

In terms of communication and fluid flow, the organization of SEDBs observed in the Aztec Sandstone serves to reduce permeability in the layers with the highest porosity. This is a desired effect that makes the reservoir more homogeneous in terms of macro-permeability. It prevents high-permeable layers to act as high-permeability flow pathways, making for more effective sweep during production, particularly during injection-assisted production. Their permeability reducing effect is not great enough (and the bands not close enough) to cause any negative effect on fluid flow.

Concluding remarks

In conclusion, the Aztec Sandstone in the Buffington Window and Valley of Fire shows what may be a characteristic development for sandstones in the contractional regime: 1) Development of distributed deformation bands with very low shear displacements (SECBs and PCBs) with no tendency to cluster to create potential future fault locations. 2) Secondary formation of strongly cataclastic band that are thinner

with larger shear offsets, also distributed but without network organization and often located at dune boundaries. This evolution is consistent with the expected deformation occurring in material hardened by both burial and pervasive distribution of SECBs (Schultz and Siddarthan, 2005; Wibberley et al., 2007). The main difference characteristics of deformation of porous sandstone in the thrusting regime are 1) the (probably early) formation of distributed deformation bands without fault localization, quite different from the more localized deformation in fault propagation folds to steeper reverse faults (Zuluaga et al. 2014) and in the extensional regime (Aydin & Johnson, 1978), and 2) the occurrence of compactional deformation bands (SECBs and PCBs), which have never been described from the extensional regime. Most of the strain and displacement, however, localized to the thrust zone, while the strain accumulated in the underlying Aztec Sandstone away from the thrust zone was very small.

Acknowledgments

This study is part of the COPS (contraction of porous sandstone) project at Center for integrated petroleum research (Uni Research CIPR), supported by the University of Bergen and Statoil.

References

Antonellini, M., Aydin, A., 1994. Effect of faulting on fluid flow in porous sandstones: petrophysical properties. American Association of Petroleum Geologists Bulletin 78, 355-377.

Aydin, A., Johnson, A. M., 1978. Development of faults as zones of deformation bands and as slip surfaces in sandstones. Pure and Applied Geophysics 116, 931-942.

Ballas, G., Soliva, R., Sizunb, J-P., Fossen, H., Benedicto, A., Skurtveit, E., 2013. Shear-enhanced compaction bands formed at shallow burial conditions; implications for fluid flow (Provence, France). Journal of Structural Geology 47, 3-15.

Ballas, G., Soliva, R., Sizun, J.-P., Benedicto, A., Cavailhes, T., Raynaud, S., 2012. The importance of the degree of cataclasis in shear bands for fluid flow in porous sandstone, Provence, France. AAPG Bulletin 96, 2167-2186.

Ballas, G., Soliva, R., Benedicto, A., Sizunb, J-P., 2014. Control of tectonic setting and large-1 scale faults on the basin-scale distribution of deformation bands in porous sandstone (Provence, France). Marine and Petroleum Geology 55, 142-159.

Bohannon, R.G., 1983. Geologic map, tectonic map, and structure sections of the Muddy and northern Black Mountains, Clark County, Nevada: U.S. Geological Survey Miscellaneous Investigations Series Map, I-1406, 1 sheet, scale 1:62,500

Brock, W.G., Engelder, J.T., 1977. Deformation associated with the movement of the Muddy Mountain overthrust in the Buffington window, southeastern Nevada. Geological Society of America Bulletin 88, 1667-1677.

Chemenda, A.I., Ballas, G., Soliva, R., 2014. Impact of a multilayer structure on initiation and evolution of strain localization in porous rocks: Field observations and numerical modeling. Tectonophysics.

Chemenda, A.I., Wibberley, C., Saillet, E., 2012, Evolution of compactive shear deformation bands: Numerical models and geological data: Tectonophysics, 526-529, 56-66.

Davis, G.H., 1999. Structural geology of the Colorado Plateau Region of southern Utah. Geological Society of America Special Paper 342, 1-157.

DeCelles, P.G., 2004. Late Jurassic to Eocene evolution of the Cordilleran thrust belt and foreland basin system, western U.S.A. American Journal of Science 304, 105-168.

Deng, S., Aydin, A., 2012. Distribution of compaction bands in 3D in an aeolian sandstone: The role of cross-bed orientation. Tectonophysics 574-575, 204-218.

Eichhubl, P., Hooker, J., Laubach, S.E., 2010. Pure and shear-enhanced compaction bands in Aztec Sandstone. Journal of Structural Geology 32, 1873-1886.

Fisher, Q.J., Knipe, R. J., 2001. The permeability of faults within siliciclastic petroleum reservoirs of the North Sea and Norwegian Continental Shelf. Marine and Petroleum Geology 18, 1063-1081.

Fossen, H., Bale, A., 2007. Deformation bands and their influence on fluid flow. American Association of Petroleum Geologists Bulletin 91, 1685-1700.

Fossen, H., Schultz, R.A., Torabi, A., 2011. Conditions and implications for compaction band formation in the Navajo Sandstone, Utah. Journal of Structural Geology 33(10), 1477-1490.

Grueschow, E., Rudnicki, J.W., 2005. Elliptic yield cap constitutive modeling for high

porosity sandstone. International Journal of Solids and Structures 42, 4574e4587

Hesthammer, J., Fossen, H., 2001. Structural core analysis from the Gullfaks area, northern North Sea. Marine and Petroleum Geology 18, 411-439.

Hubbert, M.K., Rubey, W.W., 1959. Role of fluid pressure in mechanics of over-thrust faulting. GSA Bull. 70, 115-166.

Johansen, S.E., Fossen, H., 2008. Internal geometry of fault damage zones in siliclastic rocks. In: The internal structure of fault zones: implications for mechanical and fluid-flow properties (edited by Wibberley, C. A. J., Kurz, W., Imber, J., Holdsworth, R. E. & Collettini, C.) 299. Geological Society Special Publication, 35-56.

Mollema, P.N., Antonellini, M.A., 1996. Compaction bands: a structural analog for anti-mode I cracks in aeolian sandstone. Tectonophysics 267, 209– 228.

Rives, T., Razack, M., Petit, J. P., Rawnsley, K.D., 1992. Joint spacing: analogue and numerical simulations. Journal of Structural Geology 14, 925-937.

Rotevatn, A., Torabi, A., Fossen, H., Braathen, A., 2008. Slipped deformation bands: a new type of cataclastic deformation bands in Western Sinai, Suez rift, Egypt. Journal of Structural Geology 30, 1317-1331.

Rudnicki, J. W., 2004. Shear and compaction band formation on an elliptic yield cap. Journal of Geophysical Research 109, 10.

Saillet, E., Wibberley, C.A., J. 2010. Evolution of cataclastic faulting in high-porosity sandstone, Bassin du Sud-Est, Provence, France. Journal of Structural Geology 32, 1590-1608.

Schultz, R.A., Balasko, C.M., 2003. Growth of deformation bands into echelon and ladder geometries. Journal of Geophysical Research 30.

Schultz, R.A., Siddharthan, R., 2005. A general framework for the occurrence and faulting of deformation bands in porous granular rocks. Tectonophysics 411, 1-18.

Soliva, R., Schultz, R.A., Ballas, G., Taboada, A., Wibberley, C., Saillet, E., Benedicto, A., 2013. A model of strain localization in porous sandstone as a function of tectonic setting, burial and material properties; new insight from Provence (southern France). Journal of Structural Geology 49, 50-63.

Solum, J.G., Brandenburg, J.P., Naruk, S.J., Kostenko, O.V., Wilkins, S.J., Schultz, R.A., 2010. Characterization of deformation bands associated with normal and reverse stress states in the Navajo Sandstone, Utah. American Association of Petroleum Geologists Bulletin 94, 1453-1474.

Sternlof, K., Rudnicki, J.W., Pollard, D.D., 2005. Anticrack inclusion model for compaction

bands in sandstone. Journal of Geophysical Research 110, 16.

Tembe, S., Baud, P., Wong, T.-F., 2008. Stress conditions for the propagation of discrete compaction bands in porous sandstone. Journal of Geophysical Research 113, 16.

Underhill, J. R., Woodcock, N. H., 1987. Faulting mechanisms in high-porosity sandstones: New Red Sandstone, Arran, Scotland. In: Deformation of sediments and sedimentary rocks (edited by Jones, M. E. & Preston, R. M. F.) 29. Geological Society, Special Publications, 91-105.

Wibberley, C.A.J., Petit, J.-P., Rives, T., 2007. The mechanics of fault distribution and localization in high-porosity sands, Provence, France. In: The relationship between damage and localization (edited by Lewis, H. & Couples, G. D.) 289. Geological Society, London, Special Publications, 19-46.

Wong, T.-f., Baud, P., 2012. The brittle-ductile transition in porous rock: A review. Journal of Structural Geology 44, 25-53.

Wong, T.-F., David, C., Zhu, W., 1997. The transition from brittle faulting to cataclastic flow in porous sandstones: mechanical deformation. Journal of Geophysical Research 102, 3009-3025.

Zhang, J., Wong, T.-F., Davis, D.D., 1990. Micromechanics of pressure-induced grain crushing in porous rocks. Journal of Geophysical Research 95, 341-352.

Zuluaga, L.F., Fossen, H., Rotevatn, A., 2014. Progressive evolution of deformation band populations during Laramide fault-propagation folding: Navajo Sandstone, San Rafael monocline, Utah, U.S.A. Journal of Structural Geology, 68, Part A, 66-81, ISSN 0191-8141, http://dx.doi.org/10.1016/j.jsg.2014.09.008